Contribution from the Departments of Chemistry, Thimann Laboratories, University of California, Santa Cruz, California 95064, and University of California, Davis, California 95616

Synthesis and Structural Characterization of a Trimeric Nickel(II) Complex of *N*-(2-Mercaptopropionyl)glycine

Narayan Baidya, Marilyn M. Olmstead,† and Pradip K. Mascharak*

Received December 1, 1988

Stoichiometric reaction between $[Ni(NH_3)_6]Cl_2$ and *N*-(2-mercaptopropionyl)glycine (MPG, **1**) in aqueous DMF affords a thiolato-bridged trinuclear nickel(II) complex $[Ni_3(C_5H_6NO_3S)_3]^{3-}$, which has been crystallized from MeOH/Et_2O. The complex $(NH_4)_3[Ni_3(C_5H_6NO_3S)_3]\cdot 3CH_3OH\cdot 0.5(C_2H_5)_2O$ (**3**) crystallizes in the triclinic space group $P\bar{1}$ with a = 12.707 (4) Å, b = 12.819 (8) Å, c = 14.914 (4) Å, α = 75.70 (4)°, β = 82.07 (2)°, γ = 70.31 (4)°, V = 2212 (2), and Z = 2. The structure of **3** was refined to R = 8.0% on the basis of 3944 ($I > 3\sigma(I)$) data. A novel Ni_3S_3 trigonal-antiprismatic core with an average Ni-Ni distance of 3.097 (1) Å is observed in **3**. The coordination geometry around each nickel is square planar with the thiolato S, amido N, and carboxylato O donor centers of each trianionic terdentate ligand occupying three coordination sites. The fourth site is filled by a bridging thiolato S from another ligand. The three coordination planes are ~90° to each other. The two types of Ni(II)-S interactions give rise to two distinct sets of Ni(II)-S bond lengths (~2.16 and ~2.2 Å). The average Ni(II)-N(amido) and Ni(II)-O(carboxylato) distances are 1.847 (9) and 1.904 (8) Å, respectively. The trimeric structure **3** is retained in aqueous methanolic and DMF solutions. Cleavage of thiolato bridges with additional ligand L (L = py, Im, CN^-) occurs in such solutions to produce the monomeric complexes $[Ni(C_5H_6NO_3S)L]^{n-}$ (n = 1, 2) (**4**-L). Structures of the **4**-L complexes have been elucidated by various spectroscopic techniques. All the complexes are irreversibly oxidized to unstable Ni(III) species in the potential range of +0.3 to +0.4 V vs SCE.

Introduction

Recent spectroscopic studies on the nickel-containing active site(s) of several hydrogenases have indicated the presence of S donor atoms in the first coordination sphere of the nickel center.[1-3] Elucidation of the structure and function of this low-potential S-ligated nickel site awaits exploration of structures and reactions of nickel thiolate complexes. As part of our effort in this direction, we have discovered[4] a straightforward, high-yield synthetic route to tetrahedral arenethiolates of the type $[Ni(SAr)_4]^{2-}$. We have also reported two octahedral thiolate complexes[5] that contain a $Ni^{II}N_3S_3$ chromophore and, unlike $[Ni(SAr)_4]^{2-}$, are stable in protic media. In attempts to include more biologically relevant ligands, we have isolated and structurally characterized a linear trimeric nickel(II) complex of 2-mercaptopropionic acid.[6] Since S-containing peptides will be ideal ligands for syntheses of analogues of the nickel site in the enzyme, we undertook the task of synthesizing the nickel complex(es) of the commercially available dipeptide *N*-(2-mercaptopropionyl)glycine (MPG, **1**). Similarity between the constitution of MPG and the right-hand portion of glutathione (**2**) is one clear reason for our choice.[7] In spite of

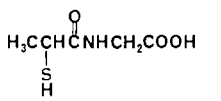

1

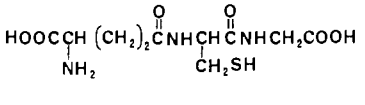

2

extensive solution studies on nickel complexes of MPG,[8-10] no definite structural information is available. We report in this paper the synthesis, structure, and spectral properties of the ammonium salt of tris(*N*-(2-mercaptopropionyl)glycinato-*O*,*N*,*S*)trinickelate(II) (**3**), a cyclic trimer in which the ligand is the triply deprotonated anion of **1** with the thiolate end bridging between two nickel centers. The solution behavior of **3** and its redox properties are also included. Apart from providing precise data on the dimensions of the coordinated MPG ligand for the first time, the present work also furnishes spectral and redox parameters of the monomeric species **4**-L (L = py, Im, CN^-), which are derived from **3** by a bridge-splitting reaction with L. The monomeric complexes **4**-L provide the unique opportunity of correlating the redox and spectral properties of a series of NiSNOX (X = S, N, O, etc.) chromophores with those of the nickel-containing active site(s) of the hydrogenases.

* To whom correspondence should be addressed at the University of California, Santa Cruz.
† University of California, Davis.

Experimental Section

Preparation of Compounds. *N*-(2-Mercaptopropionyl)glycine was purchased from Sigma Chemical Co. and used without further purification. $[Ni(NH_3)_6]Cl_2$ was synthesized by following a published procedure.[11] All operations in the following preparations were performed under a pure dinitrogen atmosphere.

$(NH_4)_3[Ni_3(C_5H_6NO_3S)_3]\cdot 3CH_3OH\cdot 0.5(C_2H_5)_2O$ (3). To a solution of 2.09 g (9 mmol) of $[Ni(NH_3)_6]Cl_2$ in 70 mL of a mixture of DMF and water (9:1) was slowly added with stirring a solution of 1.47 g (9 mmol) of MPG in 15 mL of DMF. The resultant deep reddish brown solution was stirred at 50 °C for 1 h before the volume was reduced to ca. 25 mL under vacuum. It was then filtered to remove a small amount of NH_4Cl, and to the filtrate was added 25 mL of acetonitrile. The mixture was stored at -20 °C for 12 h. The brown precipitate thus obtained was collected by filtration and recrystallized from methanol/diethyl ether. A 1.77-g (70%) batch of small dark blocks was obtained; mp 240-242 °C dec. Anal. Calcd for $C_{20}H_{47}N_6Ni_3O_{12.5}S_3$: C, 28.45; H, 5.62; N, 9.96; Ni, 20.87. Found: C, 28.21; H, 5.31; N, 10.13; Ni, 20.92. Selected IR bands (KBr pellet, cm^{-1}): 3430 (s, br), 3150 (s, br), 3000 (s, br), 1585 (s), 1560 (s), 1420 (m), 1380 (m), 1292 (w), 1245 (w), 1110 (w), 960 (m), 715 (w), 515 (w), 470 (w).

X-ray Data Collection and Reduction. Dark red plates of considerable thickness were grown by slow diffusion of diethyl ether into a dilute solution of **3** in methanol. These crystals cracked within seconds after being removed from the mother liquor, presumably due to loss of volatile molecules of crystallization (methanol and diethyl ether). In order to

(1) (a) Moura, J. J. G.; Moura, I.; Teixeira, M.; Xavier, A. V.; Fauque, G. D.; LeGall, J. *Met. Ions. Biol. Syst.* **1988**, *23*, 285. (b) Moura, J. J. G.; Teixeira, M.; Moura, I.; Xavier, A. V.; LeGall, J. In *Frontiers of Bioinorganic Chemistry*; Xavier, A. D., Ed.; VCH: Deerfield Beach, FL, 1986; p 3. (c) Moura, J. J. G.; Teixeira, M.; Moura, I.; Xavier, A. V.; LeGall, J. *J. Mol. Catal.* **1984**, *23*, 303.
(2) (a) Cammack, R. *Adv. Inorg. Chem.* **1988**, *32*, 297. (b) Albracht, S. P. J.; van der Zwaan, J. W.; Fontijn, R. D.; Slater, E. C. In *Frontiers of Bioinorganic Chemistry*; Xavier, A. V., Ed.; VCH: Deerfield Beach, FL, 1986; p 11. (c) Cammack, R.; Hall, D. O.; Rao, K. K. In *Microbial Gas Metabolism: Mechanistic, Metabolic and Biotechnological Aspects*; Poole, R. K., Dow, C., Eds., Academic: New York, 1985.
(3) (a) Hausinger, R. P. *Microbiol. Rev.* **1987**, *51*, 22. (b) Walsh, C. T.; Orme-Johnson, W. H. *Biochemistry* **1987**, *26*, 4901.
(4) Rosenfield, S. G.; Armstrong, W. H.; Mascharak, P. K. *Inorg. Chem.* **1986**, *25*, 3014.
(5) Rosenfield, S. G.; Berends, H. P.; Gelmini, L.; Stephan, D. W.; Mascharak, P. K. *Inorg. Chem.* **1987**, *26*, 2972.
(6) Rosenfield, S. G.; Wong, M. L. Y.; Stephan, D. W.; Mascharak, P. K. *Inorg. Chem.* **1987**, *26*, 4119.
(7) Results from studies on the glutathione complex will be reported elsewhere.
(8) (a) Sugiura, Y.; Hirayama, Y. *J. Am. Chem. Soc.* **1977**, *99*, 1581. (b) Sugiura, Y.; Hirayama, Y. *Inorg. Chem.* **1976**, *15*, 679. (c) Sugiura, Y.; Hirayama, Y.; Tanaka, H.; Sakurai, H. *J. Inorg. Nucl. Chem.* **1975**, *37*, 2367.
(9) Sovago, I.; Martin, R. B. *J. Inorg. Nucl. Chem.* **1981**, *43*, 425.
(10) Filella, M.; Williams, D. R. *Inorg. Chim. Acta* **1985**, *106*, 49.
(11) *Gmelins Handbuch Der Anorganischen Chemie*; Verlag Chemie: Weinheim, West Germany, 1968; Part C, Vol. 57, p 58.

0020-1669/89/1328-3426$01.50/0

Table I. Crystal Data and Data Collection and Structure Solution Parameters for $[(NH_4)_3(Ni_3[C_5H_6NO_3S]_3)]\cdot 3CH_3OH\cdot 0.5(C_2H_5)_2O$ (**3**)

formula (fw)	$C_{20}H_{47}N_6Ni_3O_{12.5}S_3$ (843.67)
color and habit	dark red plates
cryst syst	triclinic
space group	$P\bar{1}$
a, Å	12.707 (4)
b, Å	12.819 (8)
c, Å	14.914 (4)
α, deg	75.70 (4)
β, deg	82.07 (2)
γ, deg	70.31 (4)
V, Å^3	2212 (2)
Z	2
T, deg	130 K
cryst dimens, mm	0.10 × 0.38 × 0.32
d_{calc}, g cm^{-3}	1.27
d_{obsd},[a] g cm^{-3}	1.28 (1)
radiation (λ, Å)	Mo Kα (0.71069)
μ(Mo Kα), cm^{-1}	14.5
range of transm factors	0.66–0.88
diffractometer	$P2_1$, graphite monochromator
scan method	ω, 2.0° range, 1.4° offset for bkgd
scan speed, deg min^{-1}	20
2θ range, deg	0–50
octants collected	$h,\pm k,\pm l$
no. data collected	7783
no. data used in refinement	3944 [$I > 3\sigma(I)$]
no. parameters refined	384
R[b]	0.080
R_w[c]	0.088

[a] Determined by flotation in CCl_4/cyclohexane. [b] $R = \sum||F_o| - |F_c||/|F_o|$. [c] $R_w = \sum||F_o| - |F_c||w^{1/2}/\sum|F_o w^{1/2}|$

retard this process, the crystals were withdrawn from the crystal-growing tube along with the mother liquor and immediately covered with Exxon Paratone N oil on a glass slide. The slide was kept surrounded with dry ice. Under such conditions, the crystals survived several minutes while being examined under the microscope. A crystal of suitable size was mounted on a glass fiber (still under oil), and this setup was immediately placed in the cold stream of the diffractometer.[12] A slight crack developed as the crystal was cooled to 130 K. Subsequently, this crack broadened certain peaks primarily along the b crystallographic axis. The broadening was accommodated by collection of the data using a 2° ω scan. Only random fluctuations of <2% in the intensities of two standard reflections were observed during the course of data collection. Machine parameters, crystal data, and data collection parameters are summarized in Table I.

Solution and Refinement of the Structure. The structure was solved by a combination of Patterson and difference Fourier methods (SHELXTL package, revision 5.1). Scattering factors for the non-hydrogen atoms were taken from the literature tabulations.[13] Refinement was carried out by a blocked-cascade least-squares technique on F minimizing the function $\sum w(|F_o| - |F_c|)^2$ where the weight w is defined as $1/\sigma^2(F_o)$ and F_o and F_c are the observed and calculated structure factor amplitudes. In the final cycles of refinement, all the non-hydrogen atoms except those of the solvent molecules of crystallization were assigned anisotropic thermal parameters. Hydrogen atoms bonded to the carbon atoms were included at calculated positions by using a riding model, with C–H = 0.96 Å and $U_H = 1.2U_c$. An absorption correction was applied.[14] The molecules of diethyl ether and methanol are disordered. All residual electron density is in the region of these molecules. The model used has C(16)–O(10) as 1.00 MeOH, C(17)–O(11), C(22)–O(13), and C(23)–O(14) as 0.50 MeOH, C(24)–O(15) and C(25)–O(16) as 0.25 MeOH, and C(18)–C(19)–O(12)–C(20)–C(21) as 0.50 diethyl ether. The positional parameters of C(20) and C(21) were fixed at their positions on a difference map. For each molecule of methanol, the identities of the carbon and oxygen are somewhat ambiguous but agree better with the hydrogen bonding scheme as described. The following data are tabulated: positional parameters (Table II) and selected bond distances and angles (Table III). Anisotropic thermal parameters (Table S1), hydrogen atom parameters (Table S2), a list of short contacts due to hydrogen bonding (Table S3), atomic coordinates for the atoms of the

Table II. Atomic Coordinates (×10^4) and Isotropic Thermal Parameters (Å^2 × 10^3) for **3**[a]

	x	y	z	U[b]
Ni(1)	665 (1)	3786 (1)	2087 (1)	29 (1)
Ni(2)	2092 (1)	5366 (1)	2042 (1)	33 (1)
Ni(3)	2845 (1)	2879 (1)	3118 (1)	30 (1)
S(1)	2169 (2)	2357 (2)	2073 (2)	32 (1)
S(2)	1409 (3)	4884 (3)	1007 (2)	37 (1)
S(3)	3626 (2)	3901 (3)	2043 (2)	38 (1)
O(1)	51 (7)	1044 (7)	3757 (6)	45 (4)
O(2)	−2241 (7)	5228 (7)	3261 (7)	54 (4)
O(3)	−699 (7)	4933 (7)	2309 (6)	39 (3)
O(4)	−816 (8)	7775 (7)	1339 (6)	52 (4)
O(5)	1816 (8)	7215 (8)	3859 (7)	59 (4)
O(6)	2467 (7)	5989 (7)	3000 (6)	41 (3)
O(7)	4741 (7)	4014 (8)	4347 (6)	50 (4)
O(8)	1945 (8)	1862 (8)	5729 (6)	52 (4)
O(9)	2137 (6)	2159 (7)	4179 (5)	34 (3)
N(1)	25 (8)	2794 (8)	2920 (7)	38 (4)
N(2)	826 (8)	6635 (8)	1954 (7)	38 (4)
N(3)	3526 (8)	3247 (9)	3944 (7)	37 (4)
N(4)	7507 (9)	7545 (9)	2701 (7)	47 (4)
N(5)	−107 (10)	8888 (9)	4378 (8)	55 (5)
N(6)	6644 (8)	4254 (10)	4814 (6)	51 (5)
C(1)	1631 (10)	1219 (9)	2739 (8)	36 (5)
C(2)	1696 (14)	381 (13)	2141 (10)	60 (7)
C(3)	522 (10)	1671 (9)	3177 (7)	33 (4)
C(4)	−1068 (10)	3334 (11)	3312 (11)	54 (6)
C(5)	−1359 (9)	4577 (10)	2946 (9)	39 (5)
C(6)	279 (11)	6198 (10)	667 (8)	43 (5)
C(7)	526 (15)	6857 (14)	−310 (9)	65 (7)
C(8)	72 (11)	6917 (10)	1382 (8)	45 (5)
C(9)	676 (11)	7313 (10)	2628 (8)	42 (5)
C(10)	1710 (11)	6765 (10)	3219 (10)	48 (6)
C(11)	4597 (9)	4097 (12)	2748 (10)	49 (6)
C(12)	5803 (11)	3401 (16)	2520 (12)	73 (8)
C(13)	4279 (9)	3786 (11)	3747 (9)	41 (5)
C(14)	3160 (10)	2900 (11)	4929 (8)	38 (5)
C(15)	2383 (10)	2257 (10)	4958 (8)	39 (5)

[a] The coordinates for the atoms of the solvents of crystallization are included in the supplementary material. [b] Equivalent isotropic U defined as one-third of the trace of the orthogonalized U_{ij} tensor.

Table III. Selected Bond Lengths (Å) and Angles (deg) for **3**

Bond Lengths			
Ni(1)–S(1)	2.158 (3)	Ni(1)–S(2)	2.198 (3)
Ni(1)–O(3)	1.908 (7)	Ni(1)–N(1)	1.859 (10)
Ni(2)–S(2)	2.172 (4)	Ni(2)–S(3)	2.204 (3)
Ni(2)–O(6)	1.902 (10)	Ni(2)–N(2)	1.855 (9)
Ni(3)–S(1)	2.210 (4)	Ni(3)–S(3)	2.161 (3)
Ni(3)–O(9)	1.901 (7)	Ni(3)–N(3)	1.829 (12)
S(1)–C(1)	1.831 (13)	O(1)–C(3)	1.261 (15)
O(2)–C(5)	1.262 (14)	O(3)–C(5)	1.280 (15)
N(1)–C(3)	1.341 (13)	N(1)–C(4)	1.443 (15)
C(1)–C(2)	1.532 (23)	C(1)–C(3)	1.461 (16)
C(4)–C(5)	1.484 (17)	Ni(1)–Ni(2)	3.127 (1)
Ni(2)–Ni(3)	3.081 (1)	Ni(1)–Ni(3)	3.084 (1)
Bond Angles			
S(1)–Ni(1)–S(2)	91.4 (1)	S(1)–Ni(1)–O(3)	170.6 (3)
S(2)–Ni(1)–O(3)	96.8 (3)	S(1)–Ni(1)–N(1)	87.1 (3)
S(2)–Ni(1)–N(1)	174.9 (4)	O(3)–Ni(1)–N(1)	85.1 (4)
S(2)–Ni(2)–S(3)	91.1 (1)	S(2)–Ni(2)–O(6)	171.5 (3)
S(3)–Ni(2)–O(6)	96.6 (2)	S(2)–Ni(2)–N(2)	87.0 (4)
S(3)–Ni(2)–N(2)	176.0 (3)	O(6)–Ni(2)–N(2)	85.6 (4)
S(1)–Ni(3)–S(3)	91.2 (1)	S(1)–Ni(3)–O(9)	97.0 (3)
S(3)–Ni(3)–O(9)	170.5 (3)	S(1)–Ni(3)–N(3)	175.0 (3)
S(3)–Ni(3)–N(3)	86.6 (3)	O(9)–Ni(3)–N(3)	85.6 (4)
Ni(1)–S(1)–Ni(3)	89.8 (1)	Ni(1)–S(1)–C(1)	99.4 (3)
Ni(3)–S(1)–C(1)	104.6 (4)	Ni(1)–S(2)–Ni(2)	91.4 (1)
Ni(1)–S(2)–C(6)	105.9 (4)	Ni(2)–S(2)–C(6)	98.7 (5)
Ni(2)–S(3)–Ni(3)	89.8 (1)	Ni(2)–S(3)–C(11)	106.0 (4)
Ni(3)–S(3)–C(11)	98.9 (4)	Ni(1)–O(3)–C(5)	113.9 (7)
S(1)–C(1)–C(3)	111.4 (8)	Ni(1)–N(1)–C(4)	114.3 (8)
O(1)–C(3)–N(1)	121.8 (10)	C(2)–C(1)–C(3)	114.2 (13)
O(3)–C(5)–C(4)	117.6 (10)	O(1)–C(3)–C(1)	122.1 (9)

(12) Hope, H. In *Experimental Organometallic Chemistry: A Practicum in Synthesis and Characterization*; Wayda, A. L., Darensbourg, M. Y., Eds.; ACS Symposium Series 357; American Chemical Society: Washington, DC, 1987; Chapter X.
(13) Cromer, D. T.; Waber, J. T. *International Tables for X-ray Crystallography*; Kynoch: Birmingham, England, 1974; Vol. IV.
(14) Moezzi, B. Ph.D. Dissertation, University of California, Davis, 1987. The program obtains an absorption tensor from $F_o - F_c$ values.

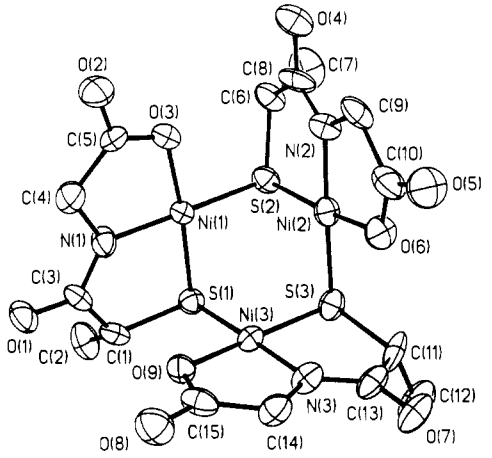

Figure 1. Computer-generated thermal ellipsoid (probability level 50%) plot of $[Ni_3(C_5H_6NO_3S)_3]^{3-}$ (anion of **3**) with the atom-labeling scheme. Hydrogen atoms are omitted for clarity.

solvents of crystallization (Table S4), and values of $10|F_o|$ and $10|F_c|$ (Table S5) have been deposited as supplementary material.

Other Physical Measurements. Absorption spectra were obtained on a Perkin-Elmer Lambda 9 spectrophotometer. ^1H and ^{13}C NMR spectra were recorded on a General Electric 300-MHz GN-300 spectrometer. The chemical shifts were measured with reference to either the HDO signal or the internal standard dioxane and are reported with reference to TMS in the text. Infrared spectra were measured on a Perkin-Elmer 1600 FTIR spectrometer. Electrochemical measurements were made with standard Princeton Applied Research instrumentation, using a glassy-carbon (GC) electrode; all potentials are referenced to an aqueous saturated calomel electrode (SCE). Elemental analysis was performed by Atlantic Microlab Inc, Atlanta, GA. Nickel was estimated gravimetrically with dimethylglyoxime.

Results and Discussion

The cyclic trimeric nickel(II) complex **3** has been isolated in high yield from the reaction mixture of $[Ni(NH_3)_6]Cl_2$ and MPG in DMF. The ammonia molecules from $[Ni(NH_3)_6]^{2+}$ presumably serve as base in generating the trianionic ligand in solution. In all previous attempts,[8-10] 3 equiv of NaOH was used for this purpose. Though several thiolato-bridged multinuclear nickel(II) complexes are known,[15] cyclic trimers of such kind are somewhat scarce. The three reported thiolato-bridged trimeric (cyclic) nickel(II) complexes, namely, $[Ni_3(\mu_3\text{-}S)(\mu\text{-}SMe)_3(SMe)_3]^{2-}$, $[Ni_3(\mu_3\text{-}S)(\mu\text{-}SPh)_3(SPh)_3]^{2-}$, and $[Ni_3(\mu_3\text{-}S)_3(o\text{-}S\{CH_2\}_2C_6H_4)_3]^{2-}$, contain μ_3-sulfido bonding.[16,17] The present complex **3**, however, is devoid of the central μ_3-S atom and comprises a unique trigonal-antiprismatic Ni_3S_3 core (vide infra). The propensity of bridge formation by thiolato sulfur is evident in the synthesis of **3**; despite the presence of additional ammonia molecules in solution, only the thiolato-bridged trimer is obtained.

Structure of $(NH_4)_3[Ni_3(C_5H_6NO_3S)_3]\cdot 3CH_3OH\cdot 0.5(C_2H_5)_2O$ (3). The crystal structure consists of discrete trimeric Ni(II) trianions and an equivalent number of NH_4^+ ions. For each formula unit, there are six methanol sites, some of which are partially occupied, and an ether molecule at approximately 0.5 occupancy. Although the solvent molecules of crystallization are ill-behaved to some extent, there is no ambiguity in the placement of the NH_4^+ ions and the structure of the trimeric complex anion. A computer-generated drawing of the anion is shown in Figure 1. Selected bond distances and angles are listed in Table III. The H atoms of each NH_4^+ ion form three strong hydrogen bonds to oxygens of the trimeric anion. Parameters for selected hydrogen bonds are tabulated in Table S3.

The coordination geometry around each nickel is essentially square planar, and the metal atom lies in the plane formed by the four donor atoms. Data on deviations from the least-squares planes of the S_2ON donor set for each nickel are included in the supplementary material. Each trianionic ligand occupies three of the four coordination sites, while the fourth one is filled by a bridging sulfur from another ligand (Figure 1). Due to the planarity of the two fused five-membered rings and the nearly 90° angle at the bridging sulfur, the overall shape of the anion appears to be derived from three perpendicular planes. This is clearly shown in Figure S1 (supplementary material). The trimeric anion has noncrystallographic 3-fold symmetry.[18] When viewed down this axis, the complex anion is observed to be chiral. Since **3** crystallizes in a triclinic space group, it is evident that there are equal numbers of left- and right-handed species in the crystal. The six-membered ring consisting of Ni and S atoms is in the chair conformation. Alternatively, these six atoms could be thought of as occupying the corners of a trigonal antiprism. Both the descriptions are readily perceived in Figure 2.

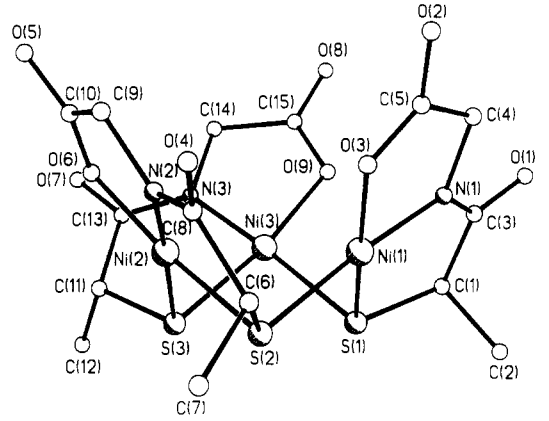

Figure 2. Perspective drawing of the anion of **3** showing the trigonal-antiprismatic Ni_3S_3 core.

Two sets of Ni(II)–S distances are observed for two kinds of Ni(II)–S bonds in **3**. The first set consists of Ni(II)–S bond lengths in individual $[Ni(C_5H_6NO_3S)]^-$ units. These distances fall in the narrow range of 2.16–2.17 Å (Table III). The second set includes lengths of the Ni(II)–S bonds that link the $[Ni(C_5H_6NO_3S)]^-$ units together to form the trimeric anion. These bonds are somewhat longer (average 2.2 Å). Similar behavior has been noted with $(Me_4N)_2[Ni_3(\mu_3\text{-}S)_3(o\text{-}S\{CH_2\}_2C_6H_4)_3]\cdot MeOH$.[17] The Ni(II)–N(amido) bond lengths in **3** lie in the range 1.83–1.88 Å and are comparable to the average Ni(II)–N(amido) bond distance of 1.99 Å in bis(glycylglycinato)nickelate(II).[19a] In nickel(II) complexes of amino acids[19b-19d] and peptides,[19a] the Ni(II)–O(carboxylato) bonds are found to be 2.0–2.2 Å long. The three Ni(II)–O(carboxylato) distances in **3** are comparatively shorter (1.9 Å). Shortening of both the Ni(II)–N(amido) and Ni(II)–O(carboxylato) bonds in the present case presumably arises from formation of two five-membered chelate rings. Significant deviations from 90° are observed with all the S–Ni–N and O–Ni–N angles (Table III) for the same reason.

Properties. Crystals of **3** dissolve in water, methanol, and DMF to give deep reddish brown solutions. Whether the trimeric structure (Figure 1) remains intact in these solutions or not is the obvious question. Since crystals of trimeric **3** are obtained by diffusion of diethyl ether into *dilute* methanolic solutions, it is quite evident that the metal-containing species in such dilute solutions is the trimer. Shown in Figure 3 are the electronic absorption spectra of **3** in aqueous borate buffer (pH 9.2) and

(15) For a recent compilation of such species, see ref 6.
(16) Matsumoto, K.; Nakano, H.; Ooi, S. *Chem. Lett.* **1988**, 823.
(17) (a) Henkel, G.; Kriege, M.; Matsumoto, K. *J. Chem. Soc., Dalton Trans.* **1988**, 657. (b) Tremel, W.; Krebs, B.; Henkel, G. *Inorg. Chim. Acta* **1983**, *80*, L31.
(18) The 3-fold axial symmetry is quite good. For example, the Ni···Ni distances average 3.097 Å with an average deviation of 0.011 Å, and the Ni···Ni···Ni angles only deviate from 60° by an average of 0.7°. Furthermore, the NiS_2ON least-squares planes are tipped equally with respect to the Ni_3 plane, with dihedral angles of 54.7, 54.2, and 55.7°. Other indicators give similar results.
(19) (a) Freeman, H. C.; Guss, J. M. *Acta Crystallogr.* **1978**, *B34*, 2451. (b) Castellano, E. E.; Nascimento, O. R.; Calvo, R. *Acta Crystallogr.* **1982**, *B38*, 1303. (c) Sakurai, T.; Iwasaki, H.; Katano, T.; Nakahashi, Y. *Acta Crystallogr.* **1978**, *B34*, 660. (d) Freeman, H. C.; Guss, J. M. *Acta Crystallogr.* **1972**, *B28*, 2090.

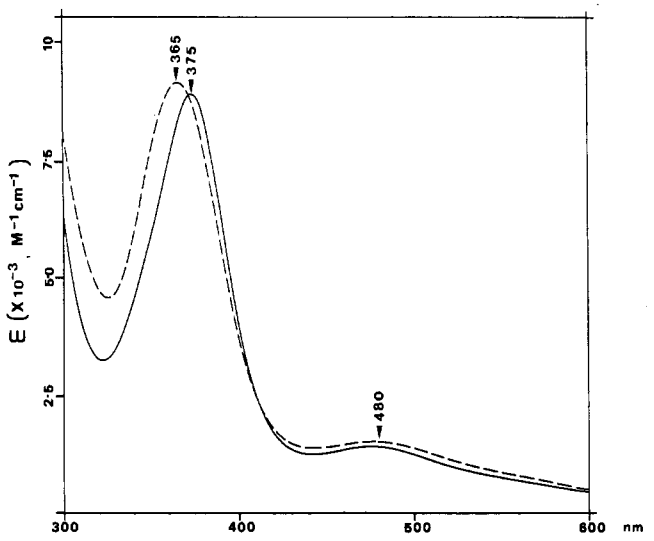

Figure 3. Absorption spectra of **3** in aqueous borate buffer, pH 9.2 (solid line), and in methanol (broken line).

Table IV. Spectroscopic and Electrochemical Data in Aqueous Borate Buffer (10 mM, pH 9.2)

Electronic Spectrum

compd	λ_{max}, nm (ϵ, M^{-1} cm^{-1})	compd	λ_{max}, nm (ϵ, M^{-1} cm^{-1})
3[a,b]	480 (1450), 375 (9000)	**4**-Im	460 (360)
4-py	460 (350)	**4**-CN	430 (360)

Peak Potential for Oxidation[c]

compd	E_p,[d] V	compd	E_p,[d] V
3	+0.38	**4**-Im	+0.32
4-py	+0.34	**4**-CN	+0.43

[a] Values quoted per trimer (i.e., 3 Ni atoms). [b] In methanol, the values are 480 (1500) and 365 (9200). [c] Differential-pulse polarography (DPP), GC electrode, 0.1 M tetraethylammonium tetafluoroborate as supporting electrolyte, modulation 25 mV peak-to-peak, 5 mV/s scan speed, clock 0.5 s. [d] Values quoted vs aqueous SCE.

methanol.[20] The spectral parameters are collected in Table IV. Except for a ca. 10-nm shift in the ~375-nm band, the absorption spectrum in methanol is very similar to that recorded in aqueous borate buffer. The similarity strongly suggests that the trimeric structure remains unchanged in aqueous buffer at pH 9.2. Absorption characteristics of **3** in aqueous buffer are pH dependent. As the pH is lowered, the intensity of both the absorption bands (Figure 3) drops sharply, showing protonation (and demetalation) of the ligand.[21] The spectrum of **3** is fully developed at pH 9.2. For this reason, the various physical measurements in aqueous medium have been performed at pH 9.2. Several reports have confirmed that, above pH 9, the trianion of MPG is coordinated to Ni^{2+} as a terdentate ligand.[8-10]

Sugiura et al.[8c] have reported a monomeric complex $[Ni(C_5H_6NO_3S)(H_2O)]^-$ (**4**-H_2O), which is synthesized from $NiCl_2 \cdot 6H_2O$, NaOH, and MPG in water. Surprisingly, the electronic

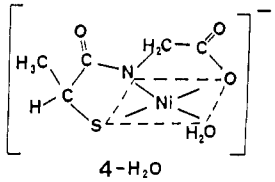

4-H_2O

absorption spectrum of this species is identical with that of **3** (see

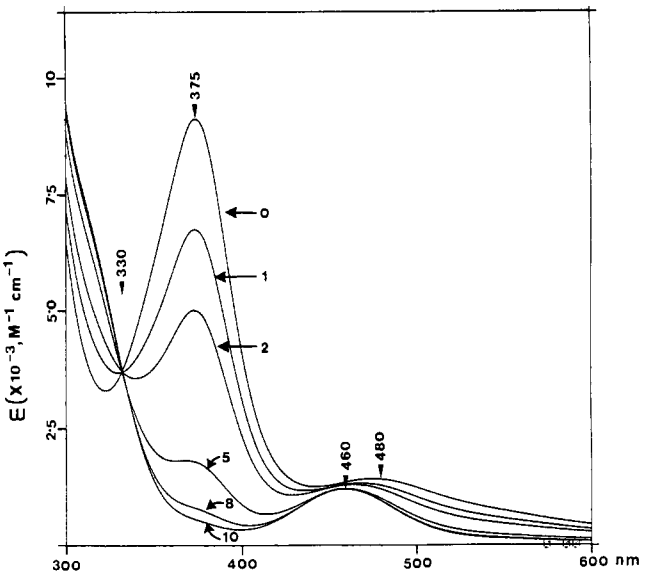

Figure 4. Changes in absorption spectrum of **3** with increasing equivalents of pyridine. Numbers next to the spectra indicate equiv of py/equiv of Ni. Formation of **4**-py is evidenced by the loss of both the 480- and the 375-nm absorptions of **3** with concomitant appearance of the 460-nm band. The limiting spectrum, i.e., the spectrum of **4**-py, is obtained with ca. 20 equiv of py/Ni (not shown here for the sake of clarity).

Figure S2, supplementary material) in borate buffer (pH 9.2). With the Ni^{2+}–MPG system, at least two groups have reported the formation of thiolato-bridged polymeric species in aqueous solution at pH >7.[9,10] Also, the ~370-nm band has been suggested to be diagnostic of the S-bridged species.[9] We have shown (vide infra) that, in the presence of additional ligand L (L = py, Im, CN^-), **3** undergoes bridge-splitting reactions to afford the **4**-L complexes, which exhibit no absorption in the region of 400–300 nm (Figure 4, Table IV). Since the proposed $[Ni(C_5H_6NO_3S)(H_2O)]^-$ species does have a strong band at 375 nm in aqueous solution with an extinct coefficient identical with that of **3**, we believe that the structure **4**-H_2O assigned by Sugiura et al. is in error. That thiolato-bridged di- or trimer could be present in basic aqueous mixtures of MPG and nickel(II) salts has been mentioned by previous workers.[9,10] Successful isolation and structure determination of **3** confirms the presence of a trimeric complex in such mixtures. We therefore propose that the complex $[Na(C_5H_6NO_3S)Ni \cdot H_2O]$ reported by Sugiura et al.[8c] should be formulated as $Na_3[Ni_3(C_5H_6NO_3S)_3] \cdot 3H_2O$.

Bridge-Splitting Reactions of 3. Cleavage of thiolato bridges in **3** with additional ligand L (eq 1) proceeds smoothly in both aqueous and nonaqueous solutions.

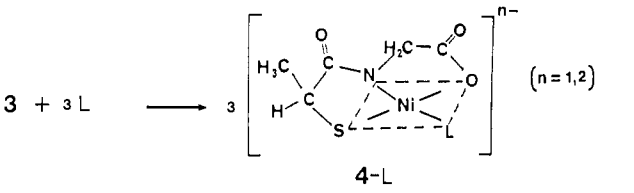

4-L

(1)

The extent of bridge-splitting depends on the donor ability of L. Reaction 1 has been studied by various spectroscopic techniques. The monomeric complex **4**-L is easily distinguished from trimeric **3** by its electronic absorption spectrum. With added L, the deep reddish brown color of **3** is rapidly changed to orange, showing formation of **4**-L, which exhibits only one moderately strong ($\epsilon \sim 350$ M^{-1} cm^{-1}) absorption band around 450 nm (Table IV). For example, when increasing equivalents of pyridine are added to a solution of **3** in aqueous borate buffer (pH 9.2), the intensities of both the 480- and the 375-nm bands are progressively reduced and new absorption due to **4**-py develops with a maximum at 460 nm (Figure 4). An isosbestic point is clearly seen at 330 nm. The limiting spectrum is obtained with ca. 20 equiv of

(20) The absorption spectrum of **3** in DMF (and DMSO) is quite similar to the ones shown in Figure 3. The ~370-nm band has a higher extinction coefficient (~11 000), however.

(21) Sovago et al.[9] have studied this aspect of Ni–MPG chemistry in detail. Our titration data are very similar to their results.

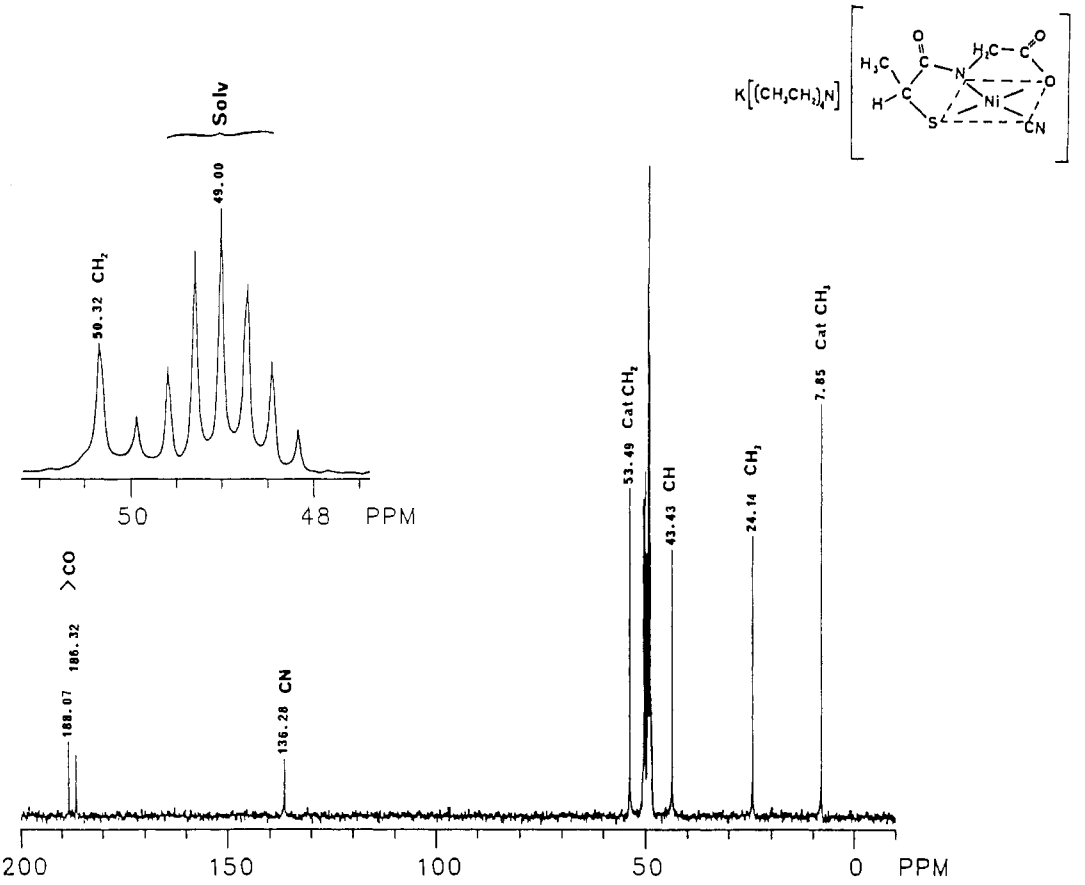

Figure 5. ^{13}C NMR spectrum (300 MHz, 292 K) of **4**-CN in CD_3OD. Signal assignments are indicated. Peak positions are referenced to TMS (see text). Inset shows the expanded plot of the ~50-ppm region. The CH_2 peak of **4**-CN appears at 50.32 ppm.

pyridine/equiv of nickel (not shown in Figure 4 for the sake of clarity). With imidazole, the limiting spectrum is reached when 5 equiv of imidazole/equiv of nickel is added to **3** in the same medium. Though imidazole appears to be a better donor in this respect, **4**-Im exhibits its absorption maximum (λ_{max}) at 460 nm. A clean cleavage reaction is observed with L = CN^-. With just 1 equiv of CN^-/equiv of nickel, **3** is rapidly converted to **4**-CN in aqueous borate buffer (pH 9.2). The stronger ligand field of CN^- is reflected in the blue shift of the λ_{max} of **4**-CN to 430 nm (Table IV). Evaporation of the reaction mixture affords dark orange microcrystals of **4**-CN,[22] which exhibits strong ν(CN) at 2110 cm^{-1} (KBr disk). The ν(CN) value confirms the presence of CN^- in the coordination sphere of nickel in **4**-CN.[23] The structure of **4**-CN has been elucidated by ^1H and ^{13}C NMR spectra (vide infra). No immediate cleavage reaction is observed with L = Cl^-. Characteristics of the bridge-splitting reaction (1) in DMF or methanol are very similar to those observed in aqueous buffer.

NMR Spectra. ^1H and ^{13}C NMR spectra of **3** in D_2O (pD 8.8) and CD_3OD are somewhat complicated and remain unassigned at present. Several unresolved broad peaks in ^1H NMR spectra as well as ^{13}C resonances of complex multiplicities most probably indicate the presence of additional multinuclear species, at higher concentration (10–15 mM). The spectral features of **4**-CN (Table V) are, however, quite straightforward. In D_2O at pD ≥9, MPG displays three sets of peaks, namely a doublet at 1.35 ppm (J = 7 Hz) for the CH_3 group, a quartet at 3.43 ppm (J = 17 Hz) for the CH group, and an AB quartet at 3.74/3.64 ppm (J_{AB} = 17 Hz) for the CH_2 group.[24] In **4**-CN, the CH group is less shielded as a result of S-coordination to nickel and resonates at 3.63 ppm. In contrast, the CH_3 doublet exhibits a high-field shift (1.26 ppm) and so does the CH_2 quartet (3.52/3.42 ppm). Since **4**-CN is generated in situ by addition of 1 equiv of CN^-/nickel to **3**, the solvent molecules of crystallization in **3** (diethyl ether and methanol) remain in solution with **4**-CN and display resonances at 1.23 and 3.08 ppm (Table V).

The ^{13}C NMR spectrum of **4**-CN in D_2O (pD 8.8) is also clean, and the various peaks (Table V) have been assigned on the basis of APT and 1PDFA data.[25] In three independent in situ generations, **4**-CN exhibited the same spectrum. Also, the spectrum remained practically unchanged in the pD range 8–11. MPG alone displays five distinct peaks in D_2O. The resonances are all shifted downfield (Table V) as the pD is raised above 8. Both APT and 1PDFA results confirm that in D_2O at pD 10, the CH_3, CH, and CH_2 carbons of anionic MPG resonate at 24.46, 37.58, and 43.60 ppm, respectively. The two low-field peaks (177.11 and 180.87 ppm) are due to the two carbonyl groups. With **4**-CN, the peaks correspondong to the two carbonyl groups are located at further downfield positions (187.76 and 185.40 ppm). Deshielding of carbonyl groups following coordination to metal has been reported.[26,27] As for the remaining three carbons of the ligand, the CH_2 and CH resonances are shifted downfield (to 49.12 and 42.32 ppm, respectively), while that for the CH_3 group is moved upfield (to 22.95 ppm). Variations in the positions of the ^{13}C resonances of MPG in D_2O with increasing pD and in **4**-CN (pD 8.8) are shown in Figure S3 (supplementary material). The CH_3 group of methanol and the CH_2 groups of diethyl ether (both originating from **3**) together give rise to the peak at 66.22 ppm.

(22) The solid analyzes satisfactorily for $K(NH_4)[Ni(C_5H_6NO_3S)CN]\cdot H_2O$. Single crystals, suitable for X-ray studies, have not been obtained at present.
(23) Nakamoto, K. In *Infrared and Raman Spectra of Inorganic and Coordination Compounds*, 4th ed.; Wiley: New York, 1986; p 272.
(24) Interestingly, the CH_2 resonance appears as a singlet (Table V) in D_2O at pD <4.
(25) Benn, R.; Gunther, H. *Angew. Chem., Int. Ed. Engl.* **1983**, *48*, 350.
(26) (a) Muetterties, M.; Cox, M. B.; Arora, S. K.; Mascharak, P. K. *Inorg. Chim. Acta* **1989**, *160*, 123. (b) Delany, K.; Arora, S. K.; Mascharak, P. K. *Inorg. Chem.* **1988**, *27*, 705.
(27) (a) Hawkins, C. J.; Martin, J. *Inorg. Chem.* **1986**, *25*, 2146. (b) Boas, L. V.; Evans, C. A.; Gillard, R. D.; Mitchell, P. R.; Phipps, D. A. *J. Chem. Soc., Dalton Trans.* **1979**, 582.

Table V. NMR Data at 292 K

^{1}H δ, ppm from TMS	^{13}C δ, ppm from TMS
MPG (D_2O, pD 3)	
1.46 (d, J = 7 Hz, 3 H), 3.63 (q, J = 7 Hz, 1 H), 3.98 (s, 2 H)	20.73, 36.60, 41.38, 173.26, 177.28
MPG (D_2O, pD 10)	
1.35 (d, J = 7 Hz, 3 H), 3.43 (q, J = 7 Hz, 1 H), 3.64/3.74 (ABq, J_{AB} = 17 Hz, 2 H)	24.46, 37.58, 43.60, 177.11, 180.87
4-CN (D_2O, pD 8.8)	
1.23 (solv, t),[a] 1.26 (d, J = 7 Hz, 3 H), 3.08 (solv, q),[a] 3.42/3.52 (ABq, J_{AB} = 17 Hz, 2 H), 3.63 (q, J = 7 Hz, 1 H)	14.33 (solv),[a] 22.95, 42.32, 49.12, 66.22 (solv),[a] 185.40, 187.76
4-CN, $K^+(Et_4N)^+$ Salt (CD_3OD)	
1.30 (m, cation), 1.20 (d, J = 7 Hz, 3 H), 2.89 (q, J = 7 Hz, 1 H), 3.30 (cation), 3.30/3.40 (ABq, J_{AB} = 20 Hz, 2 H)	7.85 (cation), 24.14, 43.43, 50.32, 53.49 (cation), 136.28, 186.32, 188.07

[a] Since **4**-CN was generated in situ by addition of 1 equiv of KCN/Ni to **3** in D_2O solution, the solvent molecules of crystallization of **3** remained in the NMR tube and gave rise to these peaks. See text and Figure 5 for signal assignments.

The CH_3 groups of diethyl ether afford the peak at 14.33 ppm. These last two assignments have been confirmed by addition of external solvents as well as APT data.

The resonance due to the coordinated CN^- in **4**-CN is not detected in D_2O at pD 8.8. The signal might be too weak or broad due to rapid exchange of coordinated CN^- with solvent and/or the slight excess of CN^- in basic solution.[28] In order to avoid these possibilities, the ^{13}C NMR spectrum of $K(Et_4N)[Ni(C_5H_6NO_3S)CN]$ ($K(Et_4N)$[**4**-CN]), first isolated by evaporation of a reaction mixture of **3**, KCN, and Et_4NBr in aqueous solution, was obtained in CD_3OD. The NMR spectrum, shown in Figure 5, does exhibit the ^{13}C resonance for the coordinated CN^- ligand at 136.29 ppm. Uncoordinated CN^- displays its ^{13}C peak at 161.80 ppm in CD_3OD. The high-field position of the CN^- peak in Figure 5 confirms that the CN^- ligand is coordinated to nickel in solution.[28] Assignments of the other resonances in Figure 5 rely on APT and 1PDFA data.

Addition of ~0.5 equiv of CN^- to an aqueous solution of **4**-CN brings about a rapid bleaching of the 430-nm absorption band, and new peaks at 24.2, 43.8, 135.5, 137, and 178.8 ppm appear in the ^{13}C NMR spectrum. These results confirm that addition of CN^- to **4**-CN leads to formation of $[Ni(CN)_4]^{2-}$ and free anionic MPG ligand in aqueous solution.[29]

Electrochemical Data. The redox properties of **3** and **4**-L (L = py, Im, CN^-) in aqueous and DMF solutions have been studied by cyclic voltammetry (CV) and differential pulse polarography (DPP). All the complexes exhibited asymmetric voltammograms, indicating irreversible oxidation to Ni(III) species. The Ni(III) species appear to undergo rapid decomposition or some subsequent reaction(s)[30] around the working electrode, since no appreciable cathodic current is detected in the reverse scan. Enhanced stability of Ni(III) complexes of peptide ligands in acidic solutions has been reported.[31] However, no improvement in CV behavior with pH is observed in the present study. The electrochemical behavior is the same on Pt and glassy-carbon (GC) electrodes and also in both protic and aprotic media.

In spite of the instability of the Ni(III) species in the present study, certain characteristics of the oxidation reactions have been determined by DPP. In aqueous borate buffer (10 mM, pH 9.2), **3** and **4**-L (L = py, Im, CN^-) display well-defined DP polarograms with a half-height width ($w_{1/2}$) of 120–180 mV.[32] The DP polarograms of **3**, **4**-Im, and **4**-CN are shown in Figure 6, and the DPP peak potentials (E_p) are collected in Table IV. In aqueous

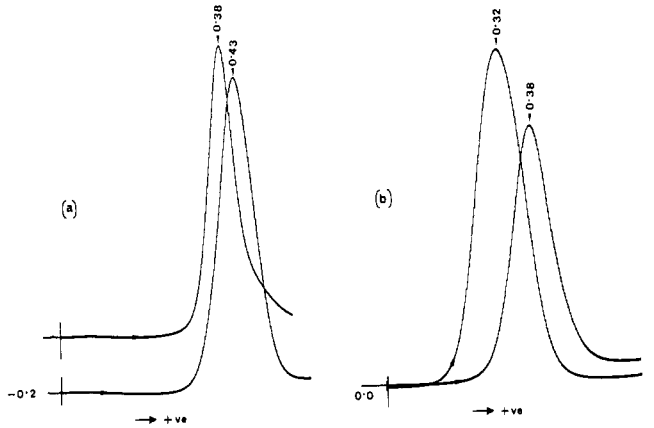

Figure 6. Differential-pulse polarograms at a GC electrode with 5 mV/s scan rate and 25-mV peak-to-peak modulation showing the oxidation of (a) **3** and **4**-CN and (b) **3** and **4**-Im in aqueous borate buffer (10 mM, pH 9.2). Peak potentials vs SCE are indicated. Note that (i) the x axes (V vs SCE) are different in the two sets and (ii) the molar concentration of **4**-L in both cases is 3 times the concentration of **3**, since **4**-L's were generated in situ by following eq 1.

borate buffer, **3** is oxidized on a GC electrode at the characteristic E_p value of +0.38 V vs SCE (Figure 6). It is of interest to note that the half-wave potential ($E_{1/2}$) for the Ni(II)/Ni(III) couple in $[Ni(H_{-2}Aib_3)]$,[33] a peptido complex with NiN_3O coordination, is +0.60 V vs SCE. The presence of thiolato S donors in the coordination sphere of nickel in **3** appears to *lower* the oxidation potential to a significant extent. A similar shift in $E_{1/2}$ values upon the substitution of in-plane anionic oxygen by thiolato sulfur donors in square-planar nickel complexes has been reported.[30a]

Oxidation of **4**-L complexes is a comparatively cleaner process. In the case of **3**, the DP polarogram is slightly asymmetric and redox processes at potentials more positive than E_p are evident in the tailing right-hand side of the polarogram (Figure 6). With **4**-L, the DP polarograms are more symmetric. The shift in E_p values of **4**-L with L (Table IV) confirms that the polarograms originate from a metal-centered redox process. Peak heights and areas under the DP polarograms[34] exhibited by various **4**-L complexes are not strictly comparable; variation in these parameters, as evident from Figure 6, presumably arises from differences in mobilities of the electroactive species. The E_p values for **4**-L complexes (Table IV) clearly indicate that in-plane coordination by N-donor ligands with delocalized π systems like py and Im does stabilize the +3 oxidation state of nickel, while CN^- provides stabilization to the +2 state. No effect of pH on the E_p values has been noted. For example, **4**-Im exhibits the same E_p value (+0.32 V vs SCE) at pH 9.2, 8.2, and 6.5. The peak current

(28) Pesek, J. J.; Mason, W. R. *Inorg. Chem.* **1983**, *22*, 2958; **1979**, *18*, 924.
(29) Under our experimental conditions (D_2O, pD 8.8), the ^{13}C signal for the CN^- ligand in $[Ni(CN)_4]^{2-}$ is observed at 137 ppm. Also, see ref 28.
(30) (a) Kruger, H.-J.; Holm, R. H. *Inorg. Chem.* **1987**, *26*, 3645. (b) Yamamura, T. *Chem. Lett.* **1986**, 801. (c) Snyder, B. S.; Rao, Ch. P.; Holm, R. H. *Aust. J. Chem.* **1986**, *39*, 963. (d) Nakabayashi, Y.; Masuda, Y.; Sekido, E. *J. Electroanal. Chem. Interfacial Electrochem.* **1986**, *205*, 209.
(31) Lappin, A. G.; McAuley, A. *Adv. Inorg. Chem.* **1988**, *32*, 241.
(32) For reversible 1-e transfer, the expected value of $w_{1/2}$ is 90 mV. See: Parry, E. P.; Osteryoung, R. A. *Anal. Chem.* **1965**, *37*, 1634.
(33) Kirksey, S. T., Jr.; Neubecker, T. A.; Margerum, D. W. *J. Am. Chem. Soc.* **1979**, *101*, 1631.
(34) That the areas under the DP polarograms approximately correspond to 1-e processes has been confirmed by using $K_4Fe(CN)_6$.

response, however, decreases steadily with decreasing pH because of loss of the electroactive species. Very similar behavior has been reported for other peptido complexes of nickel.[35] The E_p values for the **4**-L complexes in DMF are very close (±20 mV) to those recorded in aqueous borate buffer (Table IV). Since the **4**-L complexes were generated in situ for the electrochemical measurements, their electronic spectra were checked before and after the experiments to ensure integrity of the electroactive species. The E_p values and the absorption spectra of **4**-Im and **4**-py do not change appreciably with further addition of Im and py, respectively. This shows that axial coordination of L to nickel in **4**-L does not occur under the experimental conditions.[36]

Summary

The following are the principal results and conclusions of this investigation.

(1) A trimeric thiolato-bridged Ni(II) complex (**3**) of *N*-(2-mercaptopropionyl)glycine (**1**) has been isolated and structurally characterized. The complex contains a novel Ni_3S_3 trigonal-antiprismatic core. Among nickel complexes of S-containing peptides, the structure of **3** is the first one to be determined. It has been established that a previously reported complex of the composition $Na[Ni(C_5H_6NO_3S)(H_2O)]$[8c] should be formulated as $Na_3[Ni_3(C_5H_6NO_3S)_3]\cdot 3H_2O$, i.e., the Na^+ salt of **3**.

(2) Addition of L (L = py, Im, CN^-) to solutions of **3** in various protic and aprotic solvents results in bridge-splitting with concomitant generation of the monomeric complexes $[Ni(C_5H_6NO_3S)L]^{n-}$ (n = 1, 2), **4**-L. The structures of the **4**-L complexes have been elucidated by various spectroscopic techniques.

(3) Electrochemical experiments have shown that **3** and **4**-L (L = py, Im, CN^-) are irreversibly oxidized to unstable Ni(III) species in aqueous and DMF solutions. The E_p values for oxidation lie in the range of +0.30 to +0.40 V vs SCE. These values are *lower* than the usual half-wave potentials (+0.55 to +0.72 V vs SCE) observed with the various peptido complexes of nickel.

Acknowledgment. This research was supported by a grant from the Universitywide Energy Research Group of UC and a grant from UCSC "SEED" Funds at the University of California, Santa Cruz. We thank Arman Faroghi for help in the initial synthetic attempts.

Supplementary Material Available: Disposition of the three coordination planes of the three Ni centers in the anion of **3** (Figure S1), electronic absorption spectra of $Na[Ni(C_5H_6NO_3S)(H_2O)]$ and **3** in aqueous borate buffer (Figure S2), variations in the positions of the ^{13}C resonances of MPG in D_2O with increasing pD and of **4**-CN in D_2O (Figure S3), anisotropic thermal parameters for non-hydrogen atoms (Table S1), hydrogen atom parameters (Table S2), short contacts due to hydrogen bonding (Table S3), and atomic coordinates for the atoms of the solvents of crystallization (Table S4) (6 pages); values of $10|F_o|$ and $10|F_c|$ (Table S5) (24 pages). Ordering information is given on any current masthead page.

(35) Bossu, F. P.; Margerum, D. W. *Inorg. Chem.* **1977**, *16*, 1210.
(36) Murry, C. K.; Margerum, D. W. *Inorg. Chem.* **1982**, *21*, 3501.

Contribution from Ames Laboratory,[1] USDOE, and the Department of Chemistry, Iowa State University, Ames, Iowa 50011

Synthesis, Structure, and ^{31}P NMR Spectra of $Mo_2W_2Cl_8(PR_3)_4$ Rectangular Clusters

Richard T. Carlin and Robert E. McCarley*

Received November 2, 1988

The new compounds $Mo_2W_2Cl_8(PMe_3)_4\cdot C_4H_8O$ (I) and $Mo_2W_2Cl_8[P(n\text{-}Bu)_3]_4$ (II) have been prepared by cycloaddition reactions of $MoW(O_2CCMe_3)_4$. Yellow-green crystals of I provided crystallographic data for a complete structure determination: tetragonal, space group $P4_22_12$, a = 12.6443 (8) Å, c = 11.2854 (9) Å, V = 1804.3 Å^3, Z = 2, R = 0.034, R_w = 0.045. Disordering of the Mo and W atoms on the metal atom sites permits only averaged M—M, M—Cl, and M—P distances for the rectangular cluster units. Of principal interest were the M≡M and M—M distances of 2.275 (1) and 2.842 (1) Å, respectively, for the short and long edges of the Mo_2W_2 rectangular cluster units. A study of the $^{31}P\{^1H\}$ NMR spectrum for a solution of II showed that coupling of the Mo–W dinuclear units provided two isomers, IIa and IIb, in a ratio of ca. 1.5:1.0. Isomer IIa was assigned as arising from head-to-tail coupling, and IIb as arising from head-to-head coupling of the two MoW units. Electronic spectral data for II are also reported.

Introduction

The recent synthesis of the quadruply bonded dinuclear complexes $MoWCl_4(PR_3)_4$[2] sparked interest in the possibility for the preparation of the tetranuclear compounds $Mo_2W_2Cl_8(PR_3)_4$. The homonuclear analogues, $Mo_4Cl_8(PR_3)_4$[3-5] and $W_4Cl_8(PR_3)_4$,[4,5] have both been prepared. These homonuclear tetranuclear complexes have a rectangular framework of metal atoms with two unbridged, short sides and two long sides bridged by chlorines or bromines. Each metal has a distorted square-planar coordination. The bond distances in the rectangle suggest that the short, unbridged edges are M–M triple bonds and the long, halide-bridged edges are M–M single bonds.

The formation of these tetranuclear species is unique because it can be viewed as a cycloaddition of two dinuclear units.[3] This cycloaddition involves loss of the δ component of the quadruple bond in each dinuclear unit and formation of two single bonds that join the two units together.[3,6] The reaction is believed to be initiated by loss of phosphine ligand with subsequent formation of the metal–metal single bonds.[3]

Using techniques similar to those used for preparation of the homonuclear analogues,[3,5] it has been possible to synthesize $Mo_2W_2Cl_8(PMe_3)_4$ and $Mo_2W_2Cl_8(PBu_3)_4$. The characterization of these mixed-metal compounds has been accomplished by using ^{31}P NMR spectra, UV–visible spectra, and an X-ray single-crystal study.

Experimental Section

Materials. All reaction products were handled in Schlenk vessels under a nitrogen atmosphere or under vacuum. Tetrahydrofuran and cyclohexane were dried and handled as discussed earlier.[2a] Methanol was dried over sodium methoxide and vacuum-distilled onto molecular sieves (4 Å) for storage. Trimethylphosphine and tri-*n*-butylphosphine were obtained from Alpha Products and Strem Chemicals, respectively, and were used without further purification. Chlorotrimethylsilane was ob-

(1) Ames Laboratory is operated for the US Department of Energy by Iowa State University under Contract No. W-7405-Eng-82. This research was supported by the Office of Basic Energy Sciences.
(2) (a) Carlin, R. T. Ph.D. Dissertation, Iowa State University, Ames, IA, 1982; Section II. (b) Luck, R. L.; Morris, R. H.; Sawyer, J. F. *Inorg. Chem.* **1987**, *26*, 2422.
(3) Ryan, T. R.; McCarley, R. E. *Inorg. Chem.* **1982**, *21*, 2072.
(4) McCarley, R. E.; Ryan, T. R.; Torardi, C. C. *Reactivity of Metal-Metal Bonds*; Chisholm, M. H., Ed.; ACS Symposium Series 155; American Chemical Society: Washington, DC, 1981; p 41.
(5) Ryan, T. R. Ph.D. Dissertation, Iowa State University, Ames, IA, 1981; Sections II and III.
(6) Wheeler, R. A.; Hoffmann, R. *J. Am. Chem. Soc.* **1986**, *108*, 6605.

0020-1669/89/1328-3432$01.50/0